Polyethylene glycol-based bidentate ligands to enhance quantum dot and gold nanoparticle stability in biological media

Bing C Mei[1,2], Kimihiro Susumu[1], Igor L Medintz[3] & Hedi Mattoussi[1]

[1]Division of Optical Sciences, US Naval Research Laboratory, Washington, District of Columbia 20375, USA. [2]Department of Chemical Engineering, University of Massachusetts, Amherst, Massachusetts 01003, USA. [3]Center for Bio/Molecular Science and Engineering, US Naval Research Laboratory, Washington, District of Columbia 20375, USA. Correspondence should be addressed to H.M. (hedi.mattoussi@nrl.navy.mil).

Published online 5 March 2009; doi:10.1038/nprot.2008.243

We describe a simple and versatile scheme to prepare a series of poly(ethylene glycol)-based bidentate ligands that permit strong interactions with colloidal semiconductor nanocrystals (quantum dots, QDs) and gold nanoparticles (AuNPs) alike and promote their dispersion in aqueous solutions. These ligands are synthesized by coupling poly(ethylene glycol)s of various chain length to thioctic acid, followed by ring opening of the 1,2-dithiolane moiety to create a bidentate thiol anchoring group with enhanced affinity for CdSe-ZnS core-shell QDs. These ligands provide a straightforward means of preparing QDs and AuNPs that exhibit greater resistance to environmental changes, facilitating their effective use in bioassays and live cell imaging.

INTRODUCTION

Ever since the first demonstrations of QD use in biology, the drive for designing and preparing hydrophilic semiconductor nanocrystals has been intense. This is motivated by the great potential that these nanocrystals offer to overcome many of the limitations encountered by organic fluorophores and genetically engineered fluorescent proteins[1–12]. In addition to their tunable spectroscopic properties (namely absorption and emission), luminescent QDs exhibit high chemical stability, resistance to photodegradation and high photobleaching thresholds[1,4,5,13–15]. As made, the best-quality colloidal QDs (core and core-shell) are prepared by reacting organometallic precursors in coordinating solutions at high temperature, and they are soluble only in organic solvents[16–20]. This is due to the fact that the high-temperature reaction produces nanocrystals capped with ligands that are strongly hydrophobic in nature (e.g., mixtures of trioctylphosphine/trioctylphosphine oxide, TOP/TOPO and long-chain alkylamines for CdSe nanocrystals). One of the strategies to promote the transfer of these hydrophobic QDs to aqueous media involves exchanging the native caps with hydrophilic ligands, as described here[2,14,15]. Another common approach uses encapsulation of the as-prepared QDs within amphiphilic molecules, such as lipids and block-copolymers[3,4]. More recently, confining the hydrophobic QDs within the lipid bilayer of vesicles has also been proposed as a new additional route for promoting water solubility[21].

All of these approaches have advantages and disadvantages, and selection of a particular strategy should be guided by the specific application. For example, the strategy based on encapsulation within lipid micelles or block-copolymers can provide materials with relatively high quantum yields because it preserves the native ligands. It, however, tends to produce nanoparticles with larger overall radii, which may substantially increase half life circulation in blood veins and reduce renal clearance[22–25]. It may also limit its effectiveness for use in intracellular delivery and sensing through energy transfer[23–27]. Furthermore, as interactions between the amphiphilic molecules and the nanoparticles are driven by affinity between the native TOP/TOPO and the hydrophobic block of the polymer or lipid micelles (not by covalent binding), stability of the resulting nanoparticles may be weakened in certain conditions. The cap-exchange strategy provides more compact nanocrystals, which may be an advantage for size-sensitive applications; it can also facilitate intracellular uptake and renal clearance[22]. Affinity between the cap and nanoparticle surface can be strengthened by using multidentate ligands. However, it tends to produce materials with lower fluorescence quantum yields[23,25].

Surface cap exchange (driven by mass action) is relatively simple to implement and can provide QDs that are functional and small in size[23–25]. As binding to the surface is driven by coordination between the ligand anchoring head and the surface ions on the nanoparticles, not by covalent coupling, it strongly depends on the specific ligand-to-metal affinity. The binding affinity also depends on the coordination number, where multidentate ligands are expected to provide more stable interactions than monodentate ones[15]. Cap exchange has most often been applied to QDs using commercially available monothiol ligands such as those based on thiol-alkyl-carboxylic acid molecules. However, these have often produced hydrophilic nanocrystals that have short-term stability and limited accessible pH range[15,25]. These limitations are most likely due to weakness of the monodentate ligand coordination onto the nanocrystal surface. In addition, absence of a strongly hydrophilic segment within the ligand structure for commercial ligands makes the solubility dependent on the carboxyl end group, reducing the range of pHs where dispersions are stable under basic conditions[1,11,15,25].

We described in an earlier report the use of dihydrolipoic acid (DHLA) surface ligands to render CdSe-ZnS nanocrystals biocompatible[7,15]. Owing to its bidentate nature, DHLA ligands provide stable interactions with QD surfaces. This has produced aqueous QD dispersions that are stable over extended periods of time but only in basic buffers[15]; macroscopic aggregation is observed when the solution pH becomes acidic, or when the nanocrystals are mixed with cationic lipids[26]. DHLA-capped QDs also readily aggregate in the cytosol of live cells[1,5,15,26,27]. To address some of

these limitations and to further expand the range of techniques to prepare hydrophilic nanoparticles while also taking advantage of the bidentate nature of the anchoring group, we have designed a set of hydrophilic ligands that can be readily applied to semiconductor QDs and AuNPs alike[28,29].

In this protocol, we provide a detailed description of the design, preparation and purification of a series of ligands made of poly(ethylene glycol)-appended DHLA. In particular, we will present two coupling reaction schemes to prepare hydroxy-terminated and methoxy-terminated DHLA–PEG ligands. These two sets of ligands present different bonds between the dithiol head and PEG segments. The hydroxy-terminated ligands use an ester linkage, whereas the methoxy-terminated ones use an amide linkage (**Fig. 1**). We then describe the use of these ligands to perform cap exchange on CdSe-ZnS core-shell QDs as well as AuNPs and promote their transfer to aqueous media. This approach uses the bidentate chelate interactions with the nanoparticle surfaces, afforded by the dithiol on the DHLA, combined with the hydrophilic nature of the PEG chain. The presence of a PEG segment within the ligand removes the need for charged groups (i.e., carboxylic acid) to provide water solubility of the nanocrystals, as is the case with DHLA and a whole array of commercial thiol-alkyl-COOH ligands[25]. The new ligands provide nanoparticles that are stable over a broad range of pHs, and DHLA–PEG QDs are compatible with a simple conjugation strategy driven by metal–histidine affinity between CdSe-ZnS QDs and histidine-appended peptides[24]. QD–peptide conjugates prepared through this route were characterized by Förster resonance energy transfer (FRET) using dye-labeled peptide for conjugation. Self-assembled QD–peptide–dye conjugates were, for example, used as substrates for the monitoring of proteolytic enzyme activity, where specific cleavage of the peptide resulted in changes in the measured rate of FRET that depended on enzyme concentration and reaction time[30].

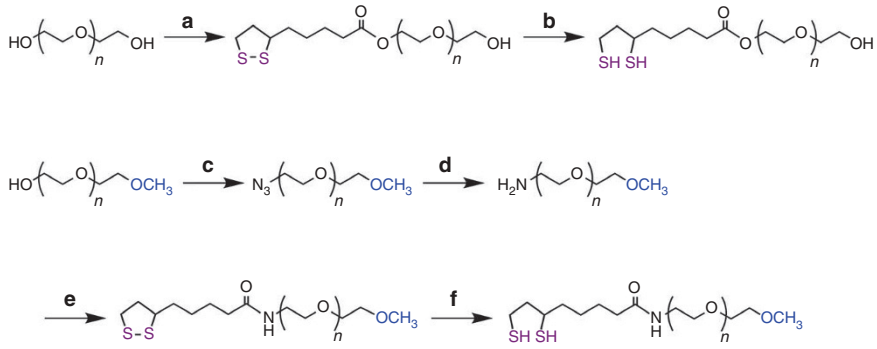

Figure 1 | Synthetic scheme. (Top) Synthetic route for preparing TA– and DHLA–PEG–OH ligands. Reagents and conditions: (**a**) DCC, DMAP, CH_2Cl_2, 0 °C → room temperature; (**b**) $NaBH_4$, EtOH/H_2O. (Bottom) Synthetic route for preparing TA– and DHLA–PEG–OCH_3 ligands. Reagents and conditions: (**c**) (i) MsCl, Et_3N, THF, (ii) NaN_3, $NaHCO_3$, H_2O; (**d**) PPh_3, THF, H_2O; (**e**) TA, DCC, DMAP, CH_2Cl_2; (**f**) $NaBH_4$, EtOH/H_2O.

Experimental design

Core-shell QDs and AuNPs. The cap-exchange strategy detailed in this protocol has been applied to both CdSe-ZnS core-shell QDs and AuNPs. The core-shell QDs that we used in our studies were prepared in our laboratory by reacting organometallic precursors at high-temperature reaction, where the CdSe cores were first grown in strong coordinating solvent mixtures of trioctylphosphine and trioctylphosphine oxide (TOP/TOPO) and alkyl amines. Several monolayers of ZnS were then grown over the cores to make CdSe-ZnS core-shell nanocrystals using the same high-temperature reaction scheme but growth was carried out at a slightly lower temperature than the one used for the core. Citrate-stabilized AuNPs used for cap exchange with our ligands were purchased from Ted Pella Inc. These can be prepared by reduction of $HAuCl_4$ with sodium citrate in water. Additional details describing the synthesis of core-shell QDs and AuNPs can be found in previous reports[16–20,31–34].

PEG-appended surface ligands. Two sets of PEG-appended thioctic acid (TA) and DHLA ligands are described in this protocol. The first, originally reported in Uyeda *et al.*[28], consists of ligands prepared by appending tunable HO–PEG–OH (PEG) segment onto TA in an esterification reaction to provide OH-terminated TA-appended PEG (TA–PEG–OH). Upon reduction of the 1,2-dithiolane group to dithiol (in the presence of $NaBH_4$), the resulting DHLA–PEG–OH ligands can be used to effectively replace the native ligands on the QDs, in a cap-exchange reaction, producing hydrophilic CdSe-ZnS nanocrystals that are stable over extended periods of time. (TA–PEG–OH does not achieve cap exchange of TOP/TOPO-QDs.) They further allowed extension of the accessible pH ranges to acidic conditions. In comparison, both TA–PEG–OH and its reduced form DHLA–PEG–OH can provide effective capping of AuNPs. However, we have recently found that reduction of the dithiolane to make DHLA–PEG–OH in the presence of excess $NaBH_4$ occasionally results in the partial decomposition of the ligand, presumably due to cleavage of the potentially labile ester bond. This has motivated the design of a second set of more resistant ligands starting from commercially available methoxy-PEG-OH (mPEG) for coupling onto TA, to produce TA–PEG–OCH_3 (see ref. 29). In a two-step reaction, the terminal hydroxy group on the mPEG was first converted to an azide, and then followed by transformation of the azide to an amine. Attachment of H_2N–PEG–OCH_3 to TA through *N,N′*-dicyclohexylcarbodiimide (DCC) coupling provided TA–PEG–OCH_3. The new TA–PEG–OCH_3 ligand differs from TA–PEG–OH in two ways: it has an amide linkage between the TA and PEG instead of the ester, and it presents an inert end group, namely methoxy instead of hydroxy. With this modification, we found that reduction of the dithiolane in the presence of even an excess (three- to fourfold) $NaBH_4$ did not alter the ligand integrity. This result is crucial in particular for performing cap exchange with semiconductor nanocrystals, which requires the reduced form of the ligand; ligand exchange with AuNPs could be realized using both TA- and DHLA-terminated ligands alike. Furthermore, by presenting a methoxy group instead of hydroxy at its lateral end, the resulting nanoparticles could potentially be more inert and less affected by nonspecific interactions. We should note that coupling of poly(ethylene glycol)s

or H_2N–PEG–OCH_3 directly onto DHLA can be used to form the final dithiol-terminated ligand. However, this route is less efficient, as the products are isolated as mixtures consisting of the reoxidized form of the ligand together with the desired product. The procedure outlined in this protocol provides higher reaction yields coupled with the ease of product separation.

Although the synthetic route should apply to various PEG chain lengths, the details described in this protocol focus on ligands having PEG400 and PEG600 (for OH-terminated ligands, where the number indicates the average MW of PEG) because they promote water solubility of QDs and AuNPs. Shorter-length ligands, such as tetraethylene glycol-appended DHLA, provide nanoparticles that are dispersible in polar solvents (e.g., methanol and ethanol) but not in water[28]. Similarly, we used commercially available mPEG550 and mPEG750 to synthesize TA–PEG–OCH_3 ligands for nanoparticle transfer to water solutions. As representative examples, the experimental procedure is limited to the synthesis of PEG600- and mPEG750-appended ligands, but the synthesis and purification schemes can be easily applied to other compounds having shorter and longer PEG or mPEG sequences. The coupling scheme between TA and PEG based on esterification is, in principle, simpler, as it involves only a single reaction through DCC coupling. However, this reaction consumes large amounts of PEG precursors because large excess ($\sim$10:1 PEG:TA ratio) is required to reduce the formation of bis-substituted PEG. In comparison, the synthesis of amide-linked TA– and DHLA–PEG–OCH_3, although requiring the additional intermediate steps from the hydroxy to an amine does not require large excess of PEG precursor as bis-substitution is eliminated. Therefore, it is much more efficient.

Controlling the nanocrystal surface reactivity. The dispersion of inorganic nanoparticles (e.g., semiconducting, metallic and magnetic) in solution environments is promoted by modification of their surfaces with ligands or block copolymers. These nanoparticles are in a size regime of 1–50 nm. They present large surfaces and consequently can accommodate high numbers of reactive groups. To achieve effective control over the nanocrystal 'reactivity' or number of functional groups, various approaches have been attempted. With the cap-exchange strategy, this can be realized by simply performing cap exchange in the presence of a ligand mixture, where a large fraction is made of inert ligands together with a smaller fraction of ligands presenting functional end groups, such as carboxyl, amine and biotin groups. These end groups provide the final nanoparticles with the desired level and type of reactivity for subsequent conjugations. For example, using carboxyl-terminated TA–PEG or DHLA–PEG in the ligand mixture, one can potentially conjugate the resulting nanoparticles to amine groups on target receptors through EDC coupling[35].

Cap exchange and nanoparticle functionality. The integrity and biological usefulness of QDs and AuNPs capped with the new ligands (DHLA–ester–PEG–OH and DHLA–amide–PEG–OCH_3) have been tested in several specific demonstrations, including general stability tests in aqueous buffers and use of these nanoparticles to develop targeted biological assays. An obvious first indication of cap exchange is the homogeneous dispersion of the nanoparticles in water, specifically for QDs, as their native TOP/TOPO cap is hydrophobic. However, citrate-stabilized AuNPs are stored in basic buffers, and dispersion in water is not sufficient to verify cap exchange. We tested the quality of the newly capped nanoparticles using three experimental approaches. The first test was based on the characterization of ligands and surface-modified nanoparticles using Fourier transform infrared (FT-IR) spectroscopy. The second focused on carrying out pH and salt stability tests of both AuNPs and CdSe-ZnS QDs alike. These are simple yet indicative tests, as the use of hydrophilic nanocrystals as tagging probes for investigating intracellular processes requires that they are stable over a broad range of pHs and salt conditions. In the third, we tested self-assembly of polyhistidine-appended peptides to the PEG-functionalized QDs (both hydroxyl- and methoxy-terminated) through metal-affinity-driven interactions. This conjugation route involves direct interactions between the histidine tag and the inorganic QD surface and was thus limited to the small and relatively extended peptides[36]. The selective conjugation between the QD donor and dye-labeled peptide (His_6-peptide-dye) can be verified by measuring changes in the rate of FRET between the QDs and dye. Increasing rate of FRET with increasing number of dyes per nanocrystal was measured for self-assembled QD–peptide–dye conjugates. We also tested the use of QD–peptide–dye conjugates as sensing assemblies (substrates) to detect the activity of specific proteases. This was achieved by measuring changes in the rate of FRET with increasing concentration of target enzyme when the peptide is recognized and cleaved by the protease. As the FRET assays are based on fluorescence detection, such experiments require small reagent concentrations (both QD and dye-labeled peptides). Experiments can be easily scaled up, provided that there is no saturation in the measured fluorescence signals.

MATERIALS

REAGENTS

! CAUTION Most of the chemicals listed below are hazardous (e.g., toxic, irritant, corrosive, flammable, lachrymator). For instance, ether and hexanes are known to be extremely flammable, tetrahydrofuran (THF) cannot be stored for a long period of time and sodium azide is toxic and can be explosive. Thus, care must be taken when handling them. THF was dried by passing through aluminum oxide before use. All the other solvents were used without further purification.

- Poly(ethylene glycol)s (average molecular weight: 400, 600 and 1,000 Da; Acros Organics)
- Poly(ethylene glycol) methyl ether (average molecular weight: 550 and 750 Da; Sigma Aldrich)
- Methanesulfonyl chloride (GFS Chemicals)
- THF (Sigma Aldrich)
- Triethylamine (Sigma Aldrich)
- Deionized water
- Sodium bicarbonate ($NaHCO_3$; Acros Organics)
- Sodium azide (NaN_3; Alfa Aesar)
- Chloroform ($CHCl_3$; Sigma Aldrich)
- Magnesium sulfate ($MgSO_4$; Sigma Aldrich)
- Methanol (MeOH; Sigma Aldrich)
- Deuterated chloroform ($CDCl_3$) with 0.03% (vol/vol) TMS (tetramethylsilane) (Cambridge Isotope Laboratories Inc.)
- Triphenylphosphine (PPh_3; Acros Organics)
- Ether (Sigma Aldrich)
- Potassium hydroxide (KOH; Acros Organics)
- Methylene chloride (CH_2Cl_2; Sigma Aldrich)
- Thioctic acid, TA (Acros Organics)
- 4-(*N*,*N*-dimethylamino)pyridine (DMAP; Acros Organics)
- DCC (Acros Organics)
- Ethyl acetate (Sigma Aldrich)
- *N*,*N*-Dimethylformamide (Sigma Aldrich)

- Deuterated dimethylsulfoxide (DMSO-d_6; Acros Organics)
- Ethanol (EtOH; Sigma Aldrich)
- Sodium borohydride ($NaBH_4$; Strem Chemicals) ▲ CRITICAL This reagent is sensitive to moisture. Storage in glove box is recommended.
- Potassium *tert*-butoxide (Sigma Aldrich) ▲ CRITICAL This reagent is sensitive to moisture. Storage in glove box is recommended.
- Hydrochloric acid (HCl; Fisher Scientific)
- Aluminum oxide (50–200 μM; Acros Organics)
- Sodium sulfate (Na_2SO_4; Sigma Aldrich)
- Celite (Sigma Aldrich)
- Silica gel (60 Å, 230–400 mesh; Bodman Industries)
- Hexanes (Sigma Aldrich)
- TOP/TOPO-capped QD in toluene[32]
- Phosphate-buffered saline (PBS; 0.138 M NaCl and 0.0027 M KCl, Sigma-Aldrich and Acros Organics)
- Sodium tetraborate buffer (pH 9.55; Sigma-Aldrich)
- Imidazole (Sigma-Aldrich)
- Acetonitrile (HPLC grade; Sigma-Aldrich)
- Citrate-stabilized AuNPs (15 nm in diameter, concentration of $\sim 1.4 \times 10^{12}$ particles ml^{-1}; Ted Pella Inc.)
- Sodium hydroxide (NaOH; Sigma Aldrich)
- Peptide sequence CSTRIDEANQRATKL$(P)_6$S$(H)_6$ (EZBioLab). The peptide is used to test the effectiveness of the metal–histine interactions with the newly capped QDs. Being a specific substrate of the enzyme, the peptide is also used in the FRET-based assay to test the proteolytic activity of trypsin
- Nickel-nitriloacetic acid agarose media (Ni-NTA; Qiagen)
- Oligonucleotide purification cartridges (OPC; Applied Biosystems). These single-use cartridges are used for desalting oligonucleotides by selective adsorption and elution on a solid-phase media (~1 ml capacity)
- Triethylamine acetate buffer (TEAA, 2 M; Applied Biosystems)
- Monoreactive Cy3-maleimide dye (Amersham Biosciences)
- Trypsin (from bovine pancreas, MW ~24 kDa; Sigma Aldrich)

EQUIPMENT

- Round-bottomed flasks, one- and two-necked
- Addition funnels
- Keck clips
- Magnetic stirring bars
- Rubber septa
- Hotplate magnetic stirrer
- Thermometers
- Distilling head
- Glass syringes and needles
- Plastic syringes and needles
- Separatory funnels
- Filter paper (Whatman qualitative circles)
- Funnels
- Rotary evaporator
- Chromatography columns (glass)
- Thin-layer column chromatography (TLC) plates (silica gel matrix with aluminum support; Sigma-Aldrich)
- Iodine chamber to stain samples on TLC
- pH test papers
- Vacuum line and nitrogen source
- NMR (Bruker SpectroSpin 400 MHz spectrometer)
- UV-visible spectrophotometer (HP 8453, Agilent Technologies)
- Fluorometer (Spex Fluorolog-3, Jobin Yvon Inc.)
- Quartz cuvettes
- Millex-LCR filters (0.45 μm pore size, hydrophilic PTFE, 25 mm diameter, nonsterile; Millipore)
- Amicon Ultra-15 centrifugal filtration units with Ultracel-50 membranes (MW cutoff ~50 kDa; Millipore)
- Centrifuges (IEC Centra CL2 centrifuge; Thermo Scientific)
- Eppendorf tubes (1.5 ml; Eppendorf International)
- PD-10 desalting gel columns (GE Healthcare)
- Mini Vortexer
- Safire dual monochromator multifunction microwell plate reader (Tecan Group Ltd)
- Low-background nonbinding microtiter 96-well plate (Corning)
- Continuum infrared microscope (Thermo Nicolet)

PROCEDURE

Synthesis of hydroxy-terminated PEG ligands

1| *Synthesis of TA–PEG600–OH: esterification reaction (Steps 1–7).* Add TA (6.19 g, 30 mmol), poly(ethylene glycol) (MW ~600 Da, 58 g, ~300 mmol), DMAP (1.1 g, 9 mmol) and dichloromethane (300 ml) in a two-necked round-bottomed flask equipped with an addition funnel, septum and a magnetic stirrer. Add DCC (6.8 g, 33 mmol) and dichloromethane (20 ml) in an addition funnel. Degas the reaction vessel with a stream of N_2 for 20 min and maintain the solution under nitrogen atmosphere until reaction is complete.

2| Cool the reaction mixture to 0 °C in an ice bath and add the DCC solution dropwise while stirring the contents. Addition of the DCC solution takes ~30 min.

3| Stir the mixture at 0 °C for 1 h. Then allow the reaction to warm gradually to room temperature (approximately 20–25 °C) and stir overnight (~18 h).
▲ CRITICAL STEP Use TLC with CH_2Cl_2:MeOH (10:1 (vol/vol)) eluent to make sure that you have the product before work-up. The spot just above the one for unreacted PEG on the TLC plate corresponds to TA–PEG600–OH; it has an R_f ~0.46.

4| Filter off the precipitate over a plug of celite and evaporate the solvent.

5| Mix the residue with a saturated aqueous sodium bicarbonate solution (200–300 ml) and extract with ethyl acetate (~100 ml) until complete extraction of TA–PEG600–OH from the aqueous layer is achieved. Completion of the extraction process can be monitored by TLC, as described for Step 3.
▲ CRITICAL STEP As extraction of TA–PEG600–OH with ethyl acetate is not very efficient, the procedure should be repeated several times (at least five times). This extraction process keeps most of the the unreacted PEG600 in the aqueous layer and makes the subsequent column purification step much easier.

6| Dry the combined organic extracts over Na_2SO_4 (~30 min or less), filter and evaporate the solvent.

7| Purify the crude product by column chromatography on silica gel with $CHCl_3$:MeOH (15:1 (vol/vol)) as the eluent and evaporate the solvent to get a yellow oil as the product. The exact details depend on the overall amount of material to be

purified. For this example, silica gel dispersed in the eluent was packed in a wide column (7.5 cm i.d.) to a height of ~30 cm. Fractions varying between 50 and 100 ml were collected as the material was eluted (under gravity), and the purity was confirmed by TLC; R_f ~0.46 for the product eluted with CH_2Cl_2: MeOH (10:1 (vol/vol)).
■ **PAUSE POINT** Compound can be stored at room temperature for at least 6 months. Storage in an inert environment (e.g., N_2) refrigerated can extend the product shelf life to 1 year.

8| *Synthesis of DHLA–PEG600-OH: reduction of the 1,2-dithiolane end group (Steps 8–11).* Dissolve TA–PEG600–OH (3.83 g, 10 mmol) in 50 ml of EtOH:water (1:4 (vol/vol)) with stirring.

9| Add $NaBH_4$ (416 mg, 11 mmol) in portions and stir for 60 min or until the solution becomes colorless under N_2.

10| Dilute the reaction mixture with brine (100 ml) and extract with $CHCl_3$ (3× 75 ml).

11| Dry the combined organic phases over Na_2SO_4, filter and evaporate the solvent.
▲ **CRITICAL STEP** This procedure requires the complete ring-opening of the 1,2 dithiolane of the TA–PEG–OH, as it is difficult to separate the reduced form of the ligand from the unreduced one. To ensure a complete reaction, use fresh $NaBH_4$ that is properly stored in an inert environment (i.e., in the glove box). Also avoid using excess $NaBH_4$, as it can lead to decomposition of the DHLA–PEG–OH; a 1:1 molar ratio of $NaBH_4$:ligand is enough to essentially achieve complete reduction without ligand degradation. The quality and purity of the final compound is best checked by ^1H NMR (see ANTICIPATED RESULTS).
■ **PAUSE POINT** The purified product is best stored under nitrogen atmosphere, in freezer. Compound is stable for at least 6 months.

Synthesis of methoxy-terminated ligands

12| *Synthesis of N_3–PEG750–OCH_3: azide modification (Steps 12–21).* Add poly(ethylene glycol) methyl ether (average MW 750 Da) (119.7 g, ~0.162 mol), THF (200 ml) and triethylamine (45 ml, 0.32 mol) to a 1-liter two-necked round-bottomed flask equipped with an addition funnel, septum and a magnetic stirring bar. Load methanesulfonyl chloride (25.0 ml, 0.32 mol) into the addition funnel. Purge the reaction vessel with nitrogen and cool the mixture to ~0 °C in an ice bath.

13| Add methanesulfonyl chloride dropwise to the reaction mixture through the addition funnel over 30 min.

14| Warm up the reaction mixture gradually to room temperature and stir overnight. Note that the reaction steps that are performed overnight are often done so for convenience, and the exact number of hours is not critical (i.e., can vary from ~12–24 h).

15| Dilute the mixture with H_2O (200 ml), and add $NaHCO_3$ (14.0 g, 0.167 mol) and sodium azide (26.3 g, 0.405 mol).

16| Attach a distilling head with a round-bottomed flask as a solvent trap. Cool the solvent trap with an ice bath. Heat the biphasic reaction mixture under N_2 to distill off the THF, and then reflux overnight.

17| Cool the reaction mixture and transfer to a separatory funnel. Extract the product multiple (approximately 3–5) times with ethyl acetate (100 ml).
▲ **CRITICAL STEP** After 3–4 extractions, use TLC with CH_2Cl_2:MeOH (10:1 (vol/vol)) to make sure that there is no product in the last ethyl acetate layer (R_f ~0.53). If the TLC shows that additional product still remains, repeat the extraction procedure until the TLC plate no longer shows the band characteristic of the N_3-PEG750–OCH_3 product.

18| Wash the combined organic layers with saturated aqueous $NaHCO_3$ solution (100–200 ml).

19| Add excess NaCl to the aqueous solution and further extract with ethyl acetate (100–200 ml) to collect additional product.

20| Dry the combined organic layers over Na_2SO_4 while stirring (~30 min), and filter through filter paper.

21| Evaporate the solvent and dry the product on a vacuum pump.
■ **PAUSE POINT** The product can be stored at room temperature and in the dark for at least 6 months. Storage in a refridgerator may extend the product's shelf life.

22| *Synthesis of H_2N–PEG750–OCH_3: amine transformation (Steps 22–29).* Dissolve N_3–PEG750–OCH_3 (72.4 g, ~9.50×10^{-2} mol) in THF (250 ml) in a 500-ml round-bottomed flask equipped with a magnetic stirring bar.

23| Add triphenylphosphine (30.0 g, 0.114 mol) and stir the reaction mixture at room temperature for 3 h under N_2.

24| Add H_2O (4.0 ml, 0.22 mol) and further stir the reaction mixture at room temperature overnight (~18 h) under N_2.

25| Evaporate the solvent using a rotary evaporator. Add ethyl acetate (250 ml) to the residue and transfer to a separatory funnel.

26| Add 1 M HCl solution (200 ml) slowly to the separatory funnel, shake and remove the organic layer. Add ethyl acetate (~200 ml) to the aqueous layer and remove the organic layer (two more times). The product should be retained in the acidic aqueous layer due to the high affinity of amino-PEG to acidic water. The purpose of the repeated wash with ethyl acetate is to remove the byproducts from the reaction.

27| Cool the aqueous layer in an ice bath and add KOH (40.0 g, 0.71 mol) slowly.

28| Extract the product with CH_2Cl_2 (100 ml, four times) and dry the combined organic layers over Na_2SO_4.

29| Filter off the Na_2SO_4 with a filter paper, evaporate the solvent using a rotary evaporator and dry the product on a vacuum pump.

■ **PAUSE POINT** Compound can be stored at room temperature in the dark (or refrigerated) in an inert environment (e.g., N_2) for at least 6 months.

30| *Synthesis of TA–PEG750–OCH_3: coupling to thioctic acid (TA) (Steps 30–39).* Add H_2N–PEG750–OCH_3 (32.8 g, ~4.46×10^{-2} mol), DMAP (1.10 g, 9.0×10^{-3} mol), DCC (9.26 g, 4.49×10^{-2} mol) and CH_2Cl_2 (150 ml) in a 500-ml round-bottomed flask equipped with an addition funnel, septa and a magnetic stirring bar. Add TA (9.20 g, 4.46×10^{-2} mol) and 50 ml of CH_2Cl_2 into the addition funnel. Cool the mixture to ~0 °C in an ice bath and purge the flask with N_2.

31| Add the TA solution dropwise while stirring over a period of ~30 min.

32| Once addition is complete, let the reaction mixture gradually warm up to room temperature while stirring overnight (approximately 10–12 h).

33| Filter the mixture through celite and rinse the celite with CH_2Cl_2.

34| Evaporate the solvent using a rotary evaporator.

35| Add water (200 ml) to the residue. Wash the aqueous mixture with ether (200 ml, three times).

36| Add $NaHCO_3$ to the aqueous solution to make it saturated. Extract the product with CH_2Cl_2 (100 ml, three times).

37| Dry the combined organic layers over Na_2SO_4, filter off Na_2SO_4 through filter paper and evaporate the solvent using a rotary evaporator.

38| Chromatograph the residue on silica gel with $CHCl_3$:MeOH (25:1 (vol/vol)) as the eluent to collect the product. The exact details depend on the overall amount of material used. In this instance, silica gel dispersed in the eluent was packed in a 5-cm (i.d.)-wide column to a height of ~30 cm. Fractions of 50–100 ml were collected as the material was eluted with gravity flow, and the purity was confirmed by TLC; R_f ~0.50 with 10:1 (vol/vol) CH_2Cl_2:MeOH.

39| Check TLC for each fraction and combine fractions with the pure product. Evaporate the solvent and dry the product under vacuum to obtain a yellow waxy solid.

■ **PAUSE POINT** The product can be stored (preferably under N_2) at room temperature in the dark for 1 year.

40| *Synthesis of DHLA–PEG750–OCH_3: reduction of 1,2-dithiolane group (Steps 40–43).* Place TA–PEG750–OCH_3 (8.821 g, ~9.54×10^{-3} mol), EtOH (15 ml) and H_2O (30 ml) in a round-bottomed flask equipped with a magnetic stirring bar and a septum. Cool the mixture in an ice bath.

41| Add $NaBH_4$ (0.78 g, 2.1×10^{-2} mol) in 10 ml of H_2O dropwise to the solution by syringe, and stir the reaction mixture at room temperature overnight (approximately 10–12 h) under N_2.

42| Add 100 ml of brine to the reaction mixture, and extract the product with CH_2Cl_2 (100 ml, three times).

43| Dry the combined organic layers over Na_2SO_4, filter off Na_2SO_4, evaporate the solvent and dry the product under vacuum to obtain a white waxy solid. The quality and purity of the final compound is best checked by ^{1}H-NMR (see ANTICIPATED RESULTS).

■ **PAUSE POINT** Compound is best stored under N_2 atmosphere in a freezer, with a shelf life of 1 year.

44| Perform the steps in Option A for cap exchange of TOP/TOPO-capped QDs with DHLA–PEG-based ligands and those in Option B for cap exchange of citrate-stabilized AuNPs with TA– and DHLA–PEG-based ligands.

(A) Cap exchange of TOP/TOPO-capped QDs with DHLA–PEG-based ligands

(i) Transfer ~500 µl of TOP/TOPO-capped QDs (growth solutions at approximately 10–50 µM) in toluene or toluene/hexano mixture to a vial. Reaction can be scaled up (i.e., we cap-exchanged up to 1 ml of TOP/TOPO-capped nanocrystals).

(ii) Precipitate the TOP/TOPO-capped QDs in toluene using excess EtOH (approximately 5—10 ml).

(iii) Centrifuge the turbid solution (for 5 min at 1,900*g* at room temperature, on IEC Centra CL2), and discard the supernatant.

? TROUBLESHOOTING

(iv) Add ~0.5 g in total of pure or mixed ligands and ~0.5 ml of EtOH to the precipitate. For mixed ligands, we have used ratios between 0 and 100% of either –COOH mixed with $-OCH_3$ (or –OH) or $-NH_2$ also mixed with $-OCH_3$ (or –OH) ligands[29].

(v) Purge the sealed vial with N_2 for approximately 5–10 min.

(vi) Heat the mixture to 60–80 °C while stirring for several hours. Although stirring the mixture for 3–4 h will be sufficient to obtain QDs that are water soluble, longer reaction times (i.e., overnight) may improve cap exchange.

(vii) Once homogenized, precipitate the sample with hexane, EtOH and $CHCl_3$ mixtures, and centrifuge the turbid solution (for 5 min at 1,900*g* at room temperature).

▲ CRITICAL STEP The ratio of hexane, EtOH and $CHCl_3$ is ~11:10:1 and may vary from batch to batch (5–10 ml total volume).

(viii) Discard the supernatant and disperse the precipitate in deionized water. In general, about 3–5 ml can be added to disperse the newly capped nanoparticles.

(ix) Pass the solution through a Millex-LCR filter.

(x) Transfer the filtrate to an Amicon Ultra-15 centrifugal filter unit.

(xi) Add deionized water up to the top line of the filter unit (~15 ml) and centrifuge (for 5 min at 1,900*g* at room temperature). Discard the filtered solution, which primarily contains excess ligand and water. The concentrated QD solution (retained in the filtration device) is usually about 0.3–0.5 ml depending on the spinning time used.

(xii) Repeat two more cycles of Step 44A(xi). To prepare the final stock solution, 1–2 ml of deionized H_2O can be added. Stock solutions with nanoparticle concentrations of approximately 5–10 µM can be stored refrigerated (~4 °C) for extended periods of time (over a year).

(xiii) Measure the absorption spectra of the QD samples. Determine the sample concentration as reported previously[37]. Stability tests (e.g., salt, pH) should be carried out as described in Experimental design and ANTICIPATED RESULTS.

(B) Cap exchange of citrate-stabilized AuNPs with TA– and DHLA–PEG-based ligands

(i) Dissolve TA– or DHLA–PEG750–OCH_3 (35 mg, ~3.7×10^{-5} mol) in 1 ml of H_2O. Note that the following procedure is for 15 nm AuNP. The amount of ligand may need to be modified for different-size nanoparticles.

(ii) Add a drop of 0.5 M NaOH into the solution to basify the mixture to pH ~10.

▲ CRITICAL STEP Check the pH of the solution with pH paper. Do not add large amounts of NaOH (pH >10), as excess counter ions will increase the likelihood of aggregation of citrate-stabilized AuNPs.

(iii) Mix the ligand solution on a stir plate and slowly add 4 ml of citrate-stabilized stock solution of AuNPs (15 nm in diameter, concentration of ~1.4×10^{12} particles ml^{-1}). Stir the dispersion overnight at a moderate speed.

(iv) Pass the dispersion through a Millex-LCR filter using a syringe.

(v) Transfer the filtrate to an Amicon Ultra-15 centrifugal filtration unit.

(vi) Add deionized H_2O up to the top line of the filter unit (~15 ml total volume) and centrifuge (for 5 min at 1,900*g* at room temperature).

? TROUBLESHOOTING

(vii) Gently shake the dispersion and centrifuge again until the volume of the remaining solution is approximately 0.25–0.3 ml.

(viii) Discard the filtered solution, which should contain excess free ligand. Repeat Steps 44B(vi) and B(vii) two more times.

(ix) Transfer the AuNP dispersion into a vial for storage and dilute as necessary.

■ PAUSE POINT Product can be stored refrigerated (4 °C) for 1 year.

(x) Measure the absorption spectra of the AuNP samples to determine the sample concentration by using the appropriate extinction coefficient. Stability tests (e.g., salt, pH) should be carried out as described in Experimental design and discussed in ANTICIPATED RESULTS.

Fluorescent labeling of the peptide

45| Dissolve peptide sequence CSTRIDEANQRATKL$(P)_6$S$(H)_6$ (~1 mg) in 10× PBS. Any peptide with His_6 (for coordination onto the QD) and a cysteine (for dye labeling) can be used[36]. The above sequence was used because it contains three trypsin-cleavable sites (two Rs and one K), making it a good candidate for assaying the enzyme.

46| Mix with two vials of Cy3-maleimide monoreactive dye and incubate overnight at 4 °C. The labeling kit, as received, contains enough dye to label 1 mg of peptide. Two vials (excess dye) are used per 1 mg of peptide to ensure complete labeling of the peptides.

TABLE 1 | FRET titration experiment.

n	0	0.15	0.25	0.5	0.75	1	1.5	2	3	4
QDs (1 μM), μl					20 (20 pmol)					
Cy3-Pep (1 μM), μl	0	3	5	10	15	20	30	40	60	80
PBS, μl	95	92	90	85	80	75	65	55	35	15

n designates the average Cy3-peptide-to-QD ratio.

47| Load the peptide–dye mixture into three columns of Ni-NTA-agarose (each with ~0.5 ml of media).

48| Wash the loaded Ni-NTA-agarose columns with 10 ml of PBS to remove excess dye. Buffer is passed through the columns under mild applied pressure using a syringe (~5 min).

49| Elute the Cy3-peptide from the Ni-NTA columns with 300 mM imidazole in PBS (~2 ml), also using a syringe.

50| Equilibrate a reverse-phase OPC by rinsing it first with 3ml of acetonitrile followed by 3 ml of 2 M TEAA buffer.

51| Load the Cy3-peptide from Step 49 into the OPC, then rinse with 0.02 M TEAA (50 ml) and subsequently with another 50 ml of deionized H_2O to remove the imidazole as well as to desalt the Cy3-peptide.

52| Elute the cleaned and desalted Cy3-peptide from the OPC with 70% acetonitrile (1–2 ml).

53| Repeat Steps 50 and 51 using the same OPC until the solution from Step 49 is clear, which indicates that all of the Cy3-peptide is extracted and desalted.

54| Measure the absorption spectra of the Cy3-peptide and quantify the amount of peptide labeled by using the extinction coefficient of the dye (i.e., 150,000 M^{-1} cm^{-1} at 553 nm for Cy3).

55| Aliquot the Cy3-peptide into Eppendorf tubes, then dry and store the samples in a desiccator at –20 °C. The exact amount depends on the application; e.g., we separated the peptide–dye solutions into five aliquots (~200 μl each).

FRET titration: self-assembly of Cy3-peptide to PEG-capped QDs

56| Calculate the volume of Cy3-peptides (at 1 μM concentration for this example) needed for each of the ten samples having a ratio, *n*, of Cy3-peptide to QDs equal to 0, 0.15, 0.25, 0.5, 0.75, 1, 1.5, 2, 3 and 4. The concentration of QDs is fixed at 20 pmol (20 μl of 1 μM solution) for this example. The following steps are written for the ratios and amounts stated in Step 56 (see **Table 1**). The concentrations and ratio can be adjusted per application, but the amount of QDs, Cy3-peptide and buffer may need to be changed accordingly.

57| Dissolve the Cy3-peptide from Step 55 in 1× PBS and prepare 300 μl of 1 μM solution. A small amount of DMSO (~1% by volume) may also be used to start dissolving the dye–peptide before buffer is added.

58| Prepare 220 μl of 1 μM DHLA–PEG QDs from Step 44(A) in 1× PBS buffer.

59| Place 20-μl aliquots of the DHLA–PEG QDs into ten Eppendorf tubes.

60| Add the appropriate amount of PBS, as per **Table 1**, to each Eppendorf tube.

61| Add the appropriate amount of 1 μM Cy3-peptide solution, as per **Table 1**, to each Eppendorf tube. Mix each sample on a vortexer once the peptide is added to ensure that the QDs are homogenously labeled.

62| Allow the samples to incubate for 5–10 min at room temperature and then place 100 μl of each sample into a microtiter 96-well plate to measure the samples' fluorescence on a plate reader.

● **TIMING**

Steps 1–7, synthesis of TA-PEG600-OH: 1.5 d
Steps 8–11, synthesis of DHLA-PEG600-OH: 3–5 h
Steps 12–21, synthesis of N_3–PEG750–OCH_3: 2 d
Steps 22–29,synthesis of H_2N–PEG750–OCH_3: 1.5 d
Steps 30–39, synthesis of TA–PEG750–OCH_3: 1.5 d
Steps 40–44, synthesis of DHLA-PEG750–OCH_3: 1 d
Step 44A, cap exchange of QDs: 1 d
Step 44B, cap exchange of AuNPs: 1 d
Steps 45–55, fluorescent labeling of peptide: 1 d
Step 56–62, FRET titration experiment: 2–4 h

? TROUBLESHOOTING

Troubleshooting advice can be found in **Table 2**.

TABLE 2 | Troubleshooting advice.

Step	Problem	Possible reason	Solution
44A(iii) and 44B(vi)	The QDs did not settle with centrifugation	The relative centrifugation force (RCF) at a given rotational speed varies with the rotor diameter. Using an IEC Centra CL2 centrifuge at 3,400 r.p.m. is approximately equal to 1,900*g*	Use the appropriate rotational speed to achieve ~1,900*g*

ANTICIPATED RESULTS

(TA–PEG600–OH)

TLC (CH_2Cl_2:MeOH = 10:1 (vol/vol)) $R_f = 0.46$.
^{1}H-NMR (400 MHz, $CDCl_3$): δ(p.p.m.) 4.18 (t, $J = 4.8$ Hz, 2H), 3.7–3.5 (m, ~50H), 3.11 (m, 2H), 2.58 (br s, 1H), 2.43 (m, 1H), 2.31 (t, $J = 7.4$ Hz, 2H), 1.87 (m, 1H), 1.7–1.55 (m, 4H), 1.5–1.35 (m, 2H).
IR (neat): 852; 949; 1,113; 1,250; 1,298; 1,350; 1,456; 1,734; 2,868 and 3,475 cm^{-1}.
Yield ~90%.

(DHLA–PEG600–OH)

^{1}H-NMR (400 MHz, $CDCl_3$): δ(p.p.m.) 4.18 (t, $J = 4.8$ Hz, 2H), 3.62 (m, ~50H), 2.88 (m, 1H), 2.66 (m, 3H), 2.31 (t, $J = 7.3$ Hz, 2H), 1.85 (m, 1H), 1.75–1.35 (m, 7H), 1.31 (t, $J = 8$ Hz, 1H), 1.26 (d, $J = 7.6$ Hz, 1H).
IR (neat): 854; 949; 1,111; 1,250; 1,298; 1,350; 1,456; 1,734; 2,553; 2,868 and 3,473 cm^{-1}.
Yield approximately 90–95%.

(TA–PEG750–OCH_3)

TLC (CH_2Cl_2:MeOH=10:1 (vol/vol)) R_f ~0.50.
^{1}H-NMR (400 MHz, in $CDCl_3$): δ(p.p.m.) 6.29 (s, 1H), 3.62–3.71 (m), 3.53–3.57 (m, 4H), 3.46 (t, 2H, $J = 5.2$ Hz), 3.38 (br s, 3H), 3.08–3.22 (m, 2H), 2.42–2.52 (m, 1H), 2.19 (t, 2H, $J = 7.2$ Hz), 1.86–1.96 (m, 1H), 1.59–1.78 (m, 4H), 1.40–1.55 (m, 2H).
IR (neat): 842; 945; 1,101; 1,244; 1,281; 1,346; 1,458; 1,536; 1,669; 2,866 and 3,334 cm^{-1}.
Yield approximately 50–60%, cumulative over the three steps.

(DHLA–PEG–OCH_3)

^{1}H-NMR (400 MHz, in $CDCl_3$): δ(p.p.m.) 6.29 (br s, 1H), 3.62–3.71 (m), 3.53–3.57 (m, 4H), 3.46 (t, 2H, $J = 5.2$ Hz), 3.38 (s, 3H), 2.92 (m, 1H), 2.6–2.8 (m, 2H), 2.20 (t, 2H, $J = 7.2$ Hz), 1.85–1.95 (m, 1H), 1.40–1.80 (m, 7H), 1.36 (t, 1H, $J = 8.0$ Hz), 1.31 (d, 1H, $J = 7.6$ Hz).
IR (neat): 850; 950; 1,108; 1,251; 1,297; 1,349; 1,456; 1,546; 1,655; 2,552; 2,872 and 3,532 cm^{-1}.
Yield approximately 90−95%.

Characterization of the newly synthesized pegylated-TA and -DHLA ligands

Characterization of both hydroxy- and methoxy-terminated PEG derivatives was carried out using ^{1}H-NMR spectroscopy[28,29]. Representative spectra shown in **Figure 2** together with the list of chemical shifts collected for all compounds indicate that the NMR features are essentially composites of those collected for the starting TA and poly(ethylene glycol) precursors. For TA–PEG–OH, the main contribution from the PEG appears as a large broad multiplet at 3.6–3.7 p.p.m., with an additional triplet (for 2H) at ~4.2 p.p.m. Upon reduction of the terminal dithiolane group, new features appear. In particular, the spectrum for the reduced form of the ligand has a well-resolved triplet and a doublet at ~1.3 and ~1.25 p.p.m., respectively, with integrated intensities of one proton each attributed to the terminal thiols[28]. In addition, resonances at ~2.9 and 2.6–2.7 p.p.m. (which are absent from TA–PEG–OH

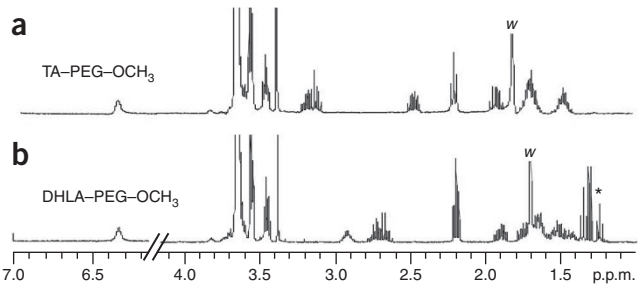

Figure 2 | ^{1}H-NMR spectra of some of the ligands. ^{1}H-NMR spectra of (**a**) TA–PEG550–OCH_3 and (**b**) DHLA–PEG550–OCH_3 in $CDCl_3$. The sharp peak (marked by *w*) around 1.8 p.p.m. is attributed to water, and the triplet at 1.25 p.p.m. is attributed to an impurity. Partially reproduced from ref. 29, with permission from the Royal Society of Chemistry (RSC).

precursor) appear for the reduced form, whereas resonances at ~3.1 and ~2.4 p.p.m. measured for the precursor are absent in the reduced ligand. Similarly, the ^{1}H-NMR data (shown in **Fig. 2**) for TA–PEG–OCH_3 indicate that the spectrum of the compound is a composite of the spectra of the two precursors (mPEG and TA), with a pronounced peak at 3.6–3.7 p.p.m. characteristic of the PEG segment, and a singlet peak at 3.38 p.p.m. attributed to the methoxy group, together with a new broad singlet peak at 6.3 p.p.m. attributed to the amide proton[28,29,35]. The ^{1}H-NMR spectrum of DHLA–PEG–OCH_3 shows an additional triplet and doublet peaks at approximately 1.3–1.4 p.p.m., attributed to the dithiol protons (**Fig. 2b**). More importantly, the amide proton peak at ~6.3 p.p.m., is maintained in the ring-opened compound. This confirms that the integrity of the coupling through the amide bond is maintained even when the 1,2-dithiolane reduction was carried out using threefold excess of $NaBH_4$.

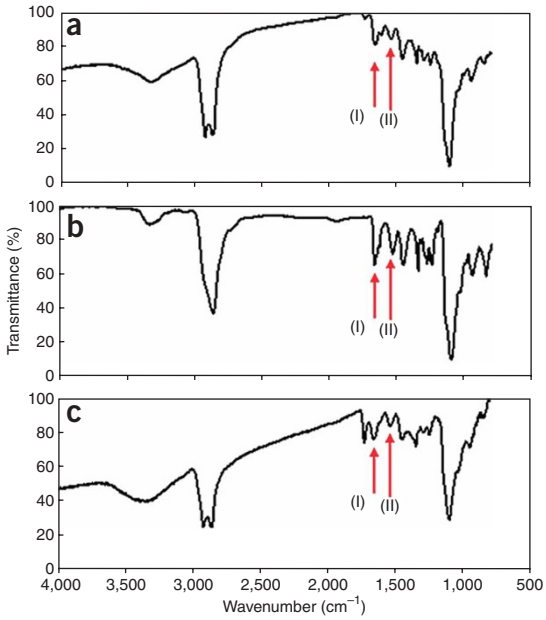

Figure 3 | FT-IR spectra of cap-exchanged QDs and AuNPs. FT-IR spectra of DHLA–PEG750–OCH_3-QDs (**a**), TA–PEG750–OCH_3 (**b**) and DHLA–PEG750–OCH_3-AuNPs (**c**). Partially reproduced from ref. 29, with permission from the Royal Society of Chemistry (RSC).

Characterization of DHLA–PEG-capped QDs

FT-IR of cap-exchanged nanoparticles. FT-IR measurements provide additional verification of whether or not following cap exchange and purification the new ligands are indeed attached to the nanoparticles. **Figure 3** shows that the IR spectra of the cap-exchanged QDs and AuNPs are similar to those of the free ligands, with all the same major bands maintained. Most notably, the spectra of cap-exchanged nanoparticles exhibit sharp bands at 1,670 cm^{-1} and 1,540 cm^{-1}, which are attributed to the amide I (C=O stretch) and amide II (N-H bending) bands from the amide bond that links the TA to mPEG, similar to the free ligand spectrum[29]. These two distinct bands are, however, present in the spectra of neither TOP/TOPO-QDs nor citrate-stabilized AuNPs. These findings confirm the effective cap exchange of the two types of nanoparticles using DHLA–PEG–OCH_3.

pH stability of nanoparticles. QDs and AuNPs capped with the mPEG-appended DHLA and TA are stable in a broad range of pH conditions and at high ionic concentrations. **Figure 4a** shows the fluorescence image for several solutions of green-emitting QDs cap-exchanged with DHLA–PEG–OCH_3 dispersed in 1× PBS over the pH range 3–13. These dispersions are stable for over 1 week; at pH 4–11, the solutions are stable for several months.

Further experiments indicate that dispersions of DHLA–PEG–OCH_3-capped AuNPs in PBS buffers were stable over the pH range 2–13 for several months, as shown in **Figure 4b**. The stability of the resulting surface-modified QDs and AuNPs with our set of ligands offers a great deal of flexibility in using these hydrophilic nanoparticles in biology. For example, the cytosol of live cells is known to have high concentrations of soluble ions and its pH is maintained acidic.

FRET characterization of QD conjugates. To demonstrate the potential utility of hydrophilic QDs prepared using the present ligand design, energy transfer experiments were conducted using DHLA–PEG (both –OH and –OCH_3)-capped QDs self-assembled with dye-labeled peptides[7,38–40]. Increasing numbers of Cy3-labeled peptides were assembled onto 530-nm emitting CdSe-ZnS QDs, through metal-histidine binding[7,35,38]. **Figure 5a** shows the PL (photoluminescence) spectra of the QD–peptide–Cy3 conjugates (excited at 300 nm) for DHLA–PEG750–OCH_3 QDs. Data show that emission from the QDs decreases, whereas that from the surface-bounded Cy3 increases with increasing number of Cy3 per conjugate, *n*. In comparison, emission from free Cy3 (to account for direct excitation at 300 nm) was negligible at all concentrations (**Fig. 5a**). Experiments carried out using DHLA–PEG600–OH QDs showed similar results. The progressive loss in QD PL combined

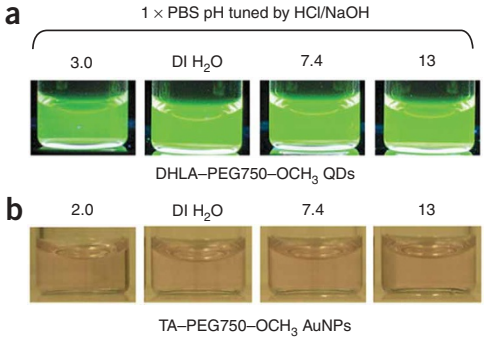

Figure 4 | pH stability of cap-exchanged nanoparticles. (**a**) Images of DHLA–PEG750–OCH_3-QDs dispersions after 1 week of storage, illuminated by a hand-held UV lamp (365 nm). (**b**) Images of TA–PEG750–OCH_3 AuNP dispersions after 3 weeks of storage, illuminated by white light. The pH of the distilled water used in these experiments is between 5.5 and 6.0. DI water, deionized water.

with the enhancement of the Cy3 emission with increasing values of n, recorded only in solutions of self-assembled QD–peptide–Cy3 conjugates, indicate that proximity-driven energy transfer between QD and dye takes place in these samples[7]. **Figure 5b** shows the normalized PL intensity of the QD and the respective FRET efficiency extracted from data in **Figure 5a**. The data were analyzed within the framework of the Förster dipole–dipole formalism and accounting for heterogeneity in conjugate valence using a Poisson distribution function[41]. The FRET efficiency can be expressed as:

$$E(n) = \sum_{k=1}^{n} p(n,k)E(k) \text{ with } p(n,k) = \frac{e^{-n}n^k}{k!},\ E(k) = \frac{kR_0^6}{kR_0^6 + r^6} \quad (1)$$

where r is the center-to-center separation distance for all dyes in these centrosymmetric conjugates, whereas n and k designate the nominal average and exact number of peptide–dye per QD conjugate, respectively; k varies between 0 and n (see refs. 30,41). The Förster radius, R_0, extracted from the absorption and emission properties of the QDs and Cy3 was ~58 Å for DHLA–PEG600–OH–QD–Cy3 and ~53 Å for DHLA–PEG750–OCH_3-QD-Cy3, respectively. The slight difference in R_0 is due to the variation of the quantum yield of the QD samples; DHLA–PEG600–OH QDs and DHLA–PEG750–OCH_3 QDs have quantum yields of ~32% and ~18%, respectively. This particular peptide contains amino acids (the C-terminal side of Lys(K) and Arg(R)) that can be specifically recognized and cleaved by the trypsin enzyme. Enzyme digestion experiments using these QD–peptide–Cy3 assemblies in the presence of a given concentration of trypsin were also conducted (data not shown). Changes in FRET rates upon cleavage of the peptide by added trypsin were measured and used to extract rates of peptide digestion, which indicates that following immobilization on the QD surface, the peptide substrates maintained their functionality and were available for digestion by the enzyme.[30] The FRET quenching experiments combined with the enzyme digestion attest to the ability of the two DHLA–PEG-capped QDs to strongly interact, through metal-affinity-driven interactions, with histidine-appended peptides, and to the fact that the resulting QD–peptide conjugates can serve as platforms for developing a variety of FRET-based assays.

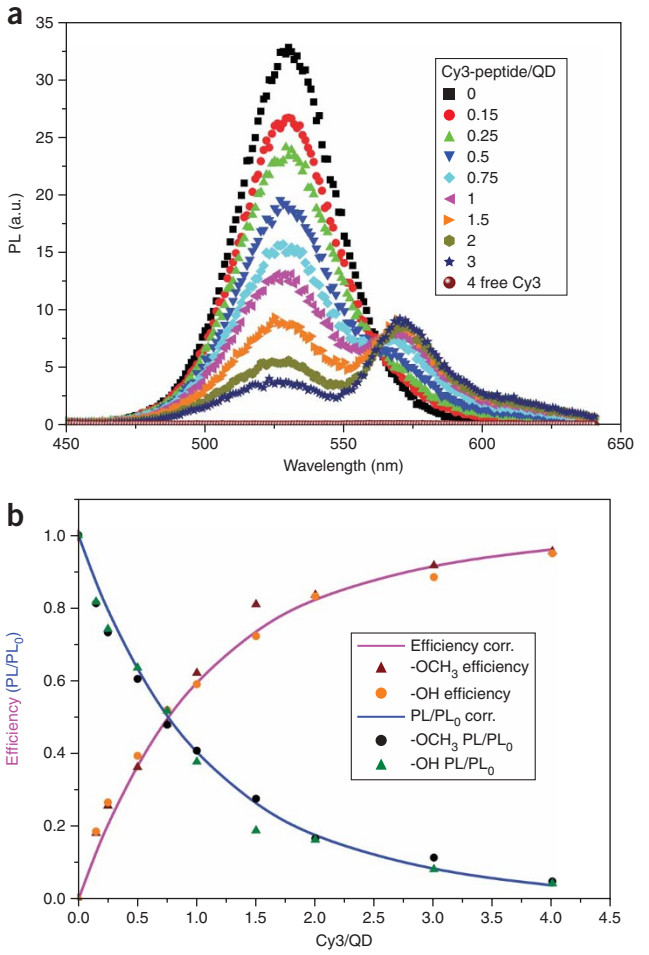

Figure 5 | Cy3-peptide titration versus 530 nm emitting QDs. (**a**) Emission spectra of Cy3-peptide–QD complexes assembled using DHLA–PEG750–OCH_3 QDs at various labeling ratios (0–3 Cy3-peptides per QD); solutions excited at 300 nm. Also shown is the direct excitation of free Cy3 without the presence of QDs as a control (solid triangles). (**b**) Normalized emission of QDs (530 nm) and FRET efficiency versus the number of Cy3-peptides per QD for both DHLA–PEG–OCH_3 and DHLA–PEG–OH-capped QDs. Also shown is the Poisson distribution-corrected fits (solid lines)[41].

ACKNOWLEDGMENTS We acknowledge NRL, Office of Naval Research (ONR), the Army Research Office (ARO) and the CB Directorate/Physical S&T Division (DTRA) for financial support. We thank Dr Horn-Bond Lin for assistance with the FTIR spectra.

Published online at http://www.natureprotocols.com/
Reprints and permissions information is available online at http://npg.nature.com/reprintsandpermissions/

1. Mattoussi, H., Kuno, M.K., Goldman, E.R., Anderson, G.P. & Mauro, J.M. Colloidal semiconductor quantum dot conjugates in biosensing. In *Optical Biosensors: Present and Future* (eds. Ligler, F.S. and Rowe Taitt, C.A.) 537–569 (Elsevier, Amsterdam, The Netherlands, 2002).
2. Åkerman, M.E., Chan, W.C.W., Laakkonen, P., Bhatia, S.N. & Ruoslahti, E. Nanocrystal targeting *in vivo*. *Proc. Natl. Acad. Sci.* **99**, 12617–12621 (2002).
3. Dubertret, B. *et al. In vivo* imaging of quantum dots encapsulated in phospholipid micelles. *Science* **298**, 1759–1762 (2002).
4. Wu, X. *et al.* Immunofluorescent labeling of cancer marker Her2 and other cellular targets with semiconductor quantum dots. *Nature Biotechnol.* **21**, 41–46 (2003).
5. Jaiswal, J.K., Mattoussi, H., Mauro, J.M. & Simon, S.M. Long-term multiple color imaging of live cells using quantum dot bioconjugates. *Nat. Biotechnol.* **21**, 47–51 (2003).
6. Goldman, E.R. *et al.* Conjugation of luminescent quantum dots with antibodies using an engineered adaptor protein to provide new reagents for fluoroimmunoassays. *Anal. Chem.* **74**, 841–847 (2002).
7. Medintz, I.L. *et al.* Self-assembled biosensors based on quantum dot FRET donors. *Nat. Mater.* **2**, 630–638 (2003).
8. Goldman, E.R. *et al.* Multiplexed toxin analysis using four colors of quantum dot fluororeagents. *Anal. Chem.* **76**, 684–688 (2004).
9. Gao, X., Cui, Y., Levenson, R.M., Chung, L.W.K. & Nie, S. *In vivo* cancer targeting and imaging with semiconductor quantum dots. *Nat. Biotechnol.* **22**, 969–976 (2004).
10. Gerion, D. *et al.* Sorting fluorescent nanocrystals with DNA. *J. Am. Chem. Soc.* **124**, 7070–7074 (2002).

11. Gerion, D. *et al.* Room-temperature single-nucleotide polymorphism and multiallele DNA detection using fluorescent nanocrystals and microarrays. *Anal. Chem.* **75**, 4766–4772 (2003).
12. Kim, S. *et al.* Near-infrared fluorescent type II quantum dots for sentinel lymph node mapping. *Nat. Biotechnol.* **22**, 93–97 (2004).
13. Bruchez, M. Jr., Moronne, M., Gin, P., Weiss, S. & Alivisatos, A.P. Semiconductor nanocrystals as fluorescent biological labels. *Science* **281**, 2013–2016 (1998).
14. Chan, W.C.W. & Nie, S. Quantum dot bioconjugates for ultrasensitive nonisotopic detection. *Science* **281**, 2016–2018 (1998).
15. Mattoussi, H. *et al.* Self-assembly of CdSe–ZnS quantum dot bioconjugates using an engineered recombinant protein. *J. Am. Chem. Soc.* **122**, 12142–12150 (2000).
16. Murray, C.B., Norris, D.J. & Bawendi, M.G. Synthesis and characterization of nearly monodisperse CdE (E=S, Se, Te) semiconductor nanocrystallites. *J. Am. Chem. Soc.* **115**, 8706–8715 (1993).
17. Hines, M.A. & Guyot-Sionnest, P. Synthesis and characterization of strongly luminescing ZnS-capped CdSe nanocrystals. *J. Phys. Chem.* **100**, 468–471 (1996).
18. Dabbousi, B.O. *et al.* (CdSe)ZnS core-shell quantum dots: synthesis and characterization of a size series of highly luminescent nanocrystallites. *J. Phys. Chem. B* **101**, 9463–9475 (1997).
19. Peng, Z.A. & Peng, X. Formation of high-quality CdTe, CdSe, and CdS nanocrystals using CdO as precursor. *J. Am. Chem. Soc.* **123**, 183–184 (2001).
20. Peng, Z.A. & Peng, X. Nearly monodisperse and shape-controlled CdSe nanocrystals via alternative routes: nucleation and growth. *J. Am. Chem. Soc.* **124**, 3343–3353 (2002).
21. Al-Jamal, W.T. *et al.* Lipid-quantum dot bilayer vesicles enhance tumor cell uptake and retention in vitro and *in vivo*. *ACS Nano* **2**, 408–418 (2008).
22. Choi, H.S. *et al.* Renal clearance of quantum dots. *Nature Biotechnol.* **25**, 1165–1170 (2007).
23. Pinaud, F., King, D., Moore, H.-P. & Weiss, S. Bioactivation and cell targeting of semiconductor CdSe/ZnS nanocrystals with phytochelatin-related peptides. *J. Am. Chem. Soc.* **126**, 6115–6123 (2004).
24. Pons, T., Uyeda, H.T., Medintz, I.L. & Mattoussi, H. Hydrodynamic dimensions, electrophoretic mobility, and stability of hydrophilic quantum dots. *J. Phys. Chem. B* **110**, 20308–20316 (2006).
25. Medintz, I.L., Uyeda, H.T., Goldman, E.R. & Mattoussi, H. Quantum dot bioconjugates for imaging, labelling and sensing. *Nat. Mater.* **4**, 435–446 (2005).
26. Voura, E.B., Jaiswal, J.K., Mattoussi, H. & Simon, S.M. Tracking metastatic tumor cell extravasation with quantum dot nanocrystals and fluorescence emission-scanning microscopy. *Nat. Med.* **10**, 993–998 (2004).
27. Jaiswal, J.K., Goldman, E.R., Mattoussi, H. & Simon, S.M. Use of quantum dots for live cell imaging. *Nat. Methods* **1**, 73–78 (2004).
28. Uyeda, H.T., Medintz, I.L., Jaiswal, J.K., Simon, S.M. & Mattoussi, H. Synthesis of compact mutidentate ligands to prepare stable hydrophilic quantum dot fluorophores. *J. Am. Chem. Soc.* **127**, 3870–3878 (2005).
29. Mei, B.C. *et al.* Modular poly(ethylene glycol) ligands for biocompatible semiconductor and gold nanocrystals with extended pH and ionic stability. *J. Mater. Chem.* **18**, 4949–4958 (2008).
30. Medintz, I.L. *et al.* Proteolytic activity monitored by fluorescence resonance energy transfer through quantum-dot–peptide conjugates. *Nat. Mater.* **5**, 581–589 (2006).
31. Qu, L., Peng, Z.A. & Peng, X. Alternative routes toward high quality CdSe nanocrystals. *Nano Lett.* **1**, 333–337 (2001).
32. Clapp, A.R., Goldman, E.R. & Mattoussi, H. Capping of CdSe-ZnS quantum dots with DHLA and subsequent conjugation with proteins. *Nat. Protoc.* **1**, 1258–1267 (2006).
33. Turkevich, J., Stevenson, P.C. & Hillier, J. A study of the nucleation and growth processes in the synthesis of colloidal gold. *Discuss. Faraday Soc.* **11**, 55–75 (1951).
34. Grabar, K.C., Freeman, R.G., Hommer, M.B. & Natan, M.J. Preparation and characterization of Au colloid monolayers. *Anal. Chem.* **67**, 735–743 (1995).
35. Susumu, K. *et al.* Enhancing the stability and biological functionalities of quantum dots via compact multifunctional ligands. *J. Am. Chem. Soc.* **129**, 13987–13996 (2007).
36. Sapsford, K.E. *et al.* Kinetics of metal-affinity driven self-assembly between proteins or peptides and CdSe-ZnS quantum dots. *J. Phys. Chem. C* **111**, 11528–11538 (2007).
37. Leatherdale, C.A., Woo, W.-K., Mikulec, F.V. & Bawendi, M.G. On the absorption cross section of CdSe nanocrystal quantum dots. *J. Phys. Chem. B* **106**, 7619–7622 (2002).
38. Clapp, A.R. *et al.* Fluorescence resonance energy transfer between quantum dot donors and dye-labeled protein acceptors. *J. Am. Chem. Soc.* **126**, 301–310 (2004).
39. Clapp, A.R. *et al.* Quantum dot-based multiplexed fluorescence resonance energy transfer. *J. Am. Chem. Soc.* **127**, 18212–18221 (2005).
40. Clapp, A.R., Medintz, I.L. & Mattoussi, H. Förster resonance energy transfer investigations using quantum-dot fluorophores. *ChemPhysChem* **7**, 47–57 (2006).
41. Pons, T., Medintz, I.L., Wang, X., English, D.S. & Mattoussi, H. Solution-phase single quantum dot fluorescence resonance energy transfer. *J. Am. Chem. Soc.* **128**, 15324–15331 (2006).